



Enhanced Channel Estimation in Multiple-Input Multiple-Output Systems: A Dual Quadratic Decomposition Algorithm Approach for Interference Cancellation



Sakkaravarthi Ramanathan^{1*}, Tirupathiah Kanaparathi², Ravi Sekhar Yarrabothu², Ramesh Sundar³

¹ Computer Science Department, Vanier College, 821 Sainte Croix Ave, Saint-Laurent, H4L 3X9 Quebec, Canada

² Department of ECE, Vignan's Foundation for Science Technology and Research (VFSTR) University, 522213 Guntur, A.P, India

³ Department of Networking and Communications, School of Computing, Faculty of Engineering and Technology, SRM Institute of Science and Technology, Kattankulathu, 603203 Chennai, India

* Correspondence: Sakkaravarthi Ramanathan (ramanats@vaniercollege.qc.ca)

Received: 07-16-2023

Revised: 08-22-2023

Accepted: 08-31-2023

Citation: S. Ramanathan, T. Kanaparathi, R. S. Yarrabothu, and R. Sundar, "Enhanced channel estimation in Multiple-Input Multiple-Output systems: A Dual Quadratic Decomposition Algorithm approach for Interference Cancellation," *Inf. Dyn. Appl.*, vol. 2, no. 3, pp. 135–142, 2023. <https://doi.org/10.56578/ida020303>.



© 2023 by the authors. Published by Acadlore Publishing Services Limited, Hong Kong. This article is available for free download and can be reused and cited, provided that the original published version is credited, under the CC BY 4.0 license.

Abstract: In Multiple-Input Multiple-Output (MIMO) systems, a considerable number of antennas are deployed at each base station, utilizing Time-shifted pilot contamination strategies. It was observed that Time-shifted pilot contamination can mitigate the adverse effects of pilot contamination, subsequently reducing Inter-group interference. However, constraints are introduced in the channel estimation process when pilots are time-shifted. To address the challenge of increasing mean square channel estimation errors in finite antenna massive MIMO systems, a novel approach using a Dual Quadratic Decomposition Algorithm for Interference Cancellation (DQDA-IC) is introduced. Through this methodology, data interference gets effectively canceled when base stations collaborate. Furthermore, compressive sensing techniques are employed, resulting in enhanced channel compensation and reduced pilot contamination in massive MIMO systems. Comparative experimental analysis, conducted using the MATLAB tool, pitted this method against two conventional techniques: Integer Linear Programming (ILP) and Q-Learning based Interference Control (QLIC). Results indicated that the DQDA-IC model surpassed its counterparts by achieving a 63% improvement in Signal to Noise Ratio (SNR), a 56% reduction in Bit Error Rate (BER), and a 92% enhancement in spectral efficiency, all within a 40 ms computational timeframe.

Keywords: Channel estimation; Massive Multiple-Input Multiple-Output (MIMO); Dual Quadratic Decomposition Algorithm for Interference Cancellation (DQDA-IC); Bit Error Rate (BER); Signal to Noise Ratio (SNR)

1 Introduction

MIMO has been recognized as a crucial component in numerous applications, with its origins traced back to third-generation (3G) wireless networks where its implementation was found to enhance the overall performance of wireless transceivers [1]. Its primary function has been identified as leveraging multiple types of antennas at both the transmitter and receiver ends, thereby boosting spectral efficiency and ensuring greater link consistency. The development of Massive MIMO systems, characterized by hundreds of antennas stationed at the base station, has been informed by insights derived from small-scale MIMO configurations [2]. Given this extensive antenna count, it was noted that base station could engage with user workstations within identical frequency bands. However, among the diverse Massive MIMO configurations, conventional variants have been observed to operate below a carrier frequency threshold of 6 GHz. In such scenarios, the aggregate number of base stations within a specified coverage area must surpass the total antenna count, a condition that has been associated with complications in the channel estimation process, primarily due to a surge in additive noise across multi-users [3].

In the context of the nascent 5G communications, similar traditional massive MIMO systems have been recorded to operate under the 6 GHz mark, with such frequencies exhibiting heightened propensities for dispersions and multipath formations [4]. Thus, it was deduced that massive MIMO might not be universally apt for all communication forms. One of the recognized advantages of array-based antennas is their straightforward implementation across

platforms, attributed primarily to the compact structure of these antennas, making them amenable to high-frequency operations [5]. Consequently, the incorporation of systems such as cmWave or mmWave within MIMO configurations is considered optimal due to their inherent propagation characteristics across channels. Challenges surrounding channel estimation in expansive multi-cellular networks have been documented [6], with primary impediments being the pronounced pilot contamination and the escalating interference from pilots discerned by users in adjacent cells. Such complexities were further attributed to the challenges presented by tasks like matrix submissions and the singular value decomposition processes when applied to extensive channel matrices [7].

Pilot contamination, being a central limitation, has been identified to introduce fading effects and environmental noise in massive MIMO configurations [8]. In the quest for a solution, the introduction of the DQDA-IC was proposed. This approach was expected to augment the model's capacity to estimate the optimal channel more efficiently. A comparative evaluation with prevalent methods such as ILP and QLIC was conducted, using parameters like BER, SNR, and timing to gauge the efficacy of the proposed technique.

2 Related Work

The importance of the Quadrature Rigid Decomposition (QRD) in the realm of MIMO receivers has been highlighted, primarily due to its foundational role in determining the reference point of the channel matrix [9]. In diverse applications, ranging from linear exposure to successive interference cancellation, the use of QRD has been documented [10]. When integrated with Sphere Converter methodologies aimed at maximizing likelihood outcomes, QRD offers a fundamental underpinning. Additionally, when combined with Successive Interference Cancellation (SIC), a comprehensive modeling of the channel covariance matrix has been integrated into the QRD, a move observed to yield significant reductions in failure rates [11]. In some studies, the employment of Substantial QRD on a regularized channel matrix was found to further mitigate error rates for SIC [12]. It was also noted that Traditional Substantial QRD could significantly curtail tree-search complexity, albeit at a minimal increase in the bit-error rate for tree-search-based detection techniques. A comparison indicated that Regularized Substantial QRD necessitated just a 50% increment in computational costs over its non-regularized counterpart [13], positioning it as an effective strategy for interference cancellation and tree-search-centric receivers.

Recent advancements in Massive MIMO systems have been introduced [14], purported to not only achieve superior gains but also to streamline requisite signal processing. In these setups, each base station is equipped in proportion to a multitude of antennas. Insights gleaned from random matrix theory and asymptotic arguments have revealed that as the quantity of antennas in a MIMO cell proliferates, inherent non-stationary noise and fading effects are nullified [15]. Moreover, the amount of users per cell remains independent of cell size, and the required transmitted energy per bit has been reported to decrease. In these massive MIMO configurations, the adoption of straightforward linear signal processing techniques, such as Matched Filter (M.F.) precoding/detection, is practiced to secure aforementioned advantages. Studies like [16] have showcased that in a massive MIMO environment, single-antenna users can proportionally reduce their transmission power relative to the total number of antennas at the base station, mirroring the performance of a singular antenna system, granted the presence of impeccable Channel State Information (CSI). Another approach, documented in [17], presents an ILP methodology, catering to minimal power requisites [18], and has been termed the "small cell network". The potential of MF-based massive MIMO systems to theoretically attain a data rate of 17 Mb/s for each user within a 20MHz channel, in both uplink and downlink trajectories, has been elaborated upon, underscoring an average throughput of 730 Mb/s per cell and a spectral efficiency of 26.5 bps/Hz [19]. Single-antenna users, it was discerned, could modulate their broadcast power, contingent on their base station antenna count [20].

Despite certain oversights, like the omission of radio front-end power consumption in the reference [21], the robustness of massive MIMO as a prime contender to elevate future network energy efficiency remains unchallenged. An exploration in the reference [22] ventured into examining diverse materials apt for the fabrication of plasmonic antennas. Findings from this research posited that Terahertz (THz) antennas crafted from graphene as a conducting medium exhibited superior electrical properties over those constituted from materials like copper or carbon nanotubes. Further investigations, as chronicled in the reference [23], delved into the resonant modes precipitated by THz plasmonic antennas, concluding that graphene-based antennas are prime candidates for the creation of compact, high-efficiency antennas. Additionally, a study in the reference [24] described a metamaterial-based THz antenna, founded on a microstrip patch antenna, fashioned on a quartz dielectric substrate, reiterating the suitability of graphene for THz antenna development. While the prior research emphasized the role of the MIMO system in channel estimation, the efficiency of the existing models was found wanting. It was suggested that an ancillary technique might be essential to enhance the performance of the MIMO system.

3 System Model

In the model under consideration, a 4×4 MIMO system is examined, which, through the implementation of DQDA-IC, can be decomposed into two distinct 2×2 systems for efficacious MIMO detection. Within this network,

various sub-cells, including microcells, picocells, and femtocells, are deployed. A representation involving the Mobile Terminal (M.T.) has been utilized to model the network under a singular cell-picocell configuration. As depicted in Figure 1, the transmitter is constructed with multiple nodes, each housing two antennas in both the Macrocell and the Picocell. Conversely, the M.T. serves as a receiver, equipped with four antennas.

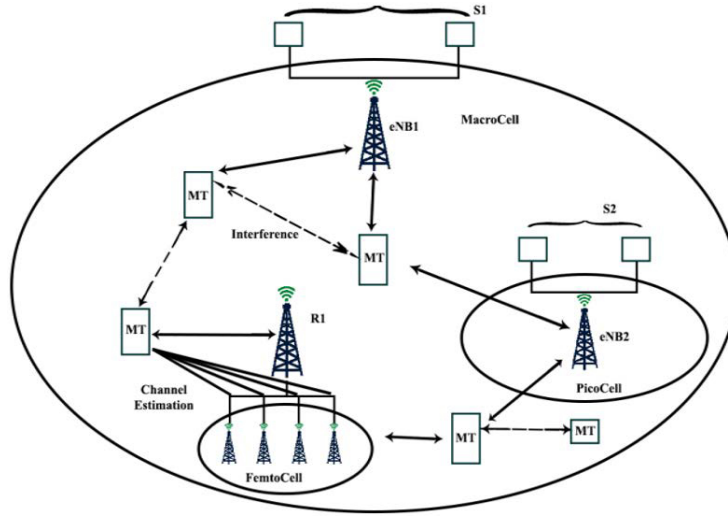


Figure 1. System model illustrating device deployment in massive MIMO

Data transmitted from eNB1 and eNB2 is denoted by S1 and S2, respectively. Here, S2 is identified as the desired data stream, while S1 signifies the interfering stream. However, when communication occurs between the M.T. and the MacroCell, S2 becomes the interference area, and S1 is recognized as the desired data stream. A primary motivation behind this research, which emphasizes the deployment of the Massive MIMO technique, is derived from its potential to amplify network efficiency and augment its capacity. The technique further permits the incorporation of a substantial number of antennas at the Base Station (BS) to cater to a diverse user base. Notably, this approach is capable of handling both digital and analog signals. Moreover, it has been observed that signals are transferred to the designated nodes with greater precision and minimal loss compared to traditional MIMO systems. The subsequent section provides an in-depth discussion on the step-by-step methodology of the proposed model.

3.1 Channel Model in Flat Fading Environments

The Nakagami channel, in conjunction with a symbol-synchronized form of the mmWave massive scheme, has been employed, featuring M and N as the numbers of transmit and receive antennas, respectively. This implies that M distinct transmissions are multiplexed on the transmission end and subsequently demultiplexed across N receivers—a procedure recognized as spatial multiplexing. When all transmissions are aggregated into vectors, the architecture can be visualized as transmitting an M_1 vector through an $N \times M$ channel matrix denoted as “ H ”. Furthermore, it has been observed that each receiver encompasses an additional intrinsic noise source. The baseband model outcome is articulated as:

$$y = Hs + n \quad (1)$$

In Eq. (1), s represents the $N \times 1$ received vector, while n delineates the noise vector. The matrix H also comprises elements, such as the (i, j) th element with the parabolic variable h_{ij} , which estimates the channel’s intricacy from a specific transmit antenna to the i th receive antenna. Additionally, a zero-mean Gaussian vector, denoted as n , with $R_n = E_{nn}^* = \sigma^2 nI$ (covariance matrix), is integrated.

The primary objective of the mmWave massive MIMO detection is channel prediction, as delineated in Eq. (2). Subsequent to the execution of Eq. (2), the DQDA-IC was devised to mitigate interference. The performance efficacy of the proposed MIMO system, utilizing DQDA-IC-based channel estimation, will be elaborated in subsequent sections.

$$\hat{s} = \arg \min_{s \in \Lambda^c} \|y - Hs\|^2 \quad (2)$$

3.2 Channel Estimation via Interference Cancellation

In the context of mmWave massive MIMO, the proposed DQDA-IC is delineated across three distinct phases. Initially, a selection is executed. This precedes the second phase, characterized as the Quadratic constraint selection.

Subsequently, in the third phase, specific constraint processes are undertaken wherein values for the chosen constraints are established; notably, when $Q = 1$, Interference Cancellation (I.C.) is achieved. Given favorable network conditions, this constraint mechanism obviates the necessity for the entire system to engage in intricate discovery processes. The blocking parameter, represented as nb , dictates the channel's decomposition into blocks. Customarily, it is chosen such that the size of n remains inferior to the channel matrix " H ", essential for executing DQDA-IC within a networked environment.

The primary aim of I.C. is to amplify the ratio of freedom ϕ^α to secure an optimal signal transmission pathway. Should T^α serve to represent the transmitted signal, its expression is derived in Eq. (3):

$$T^\alpha = \sum_{i=1}^{\phi^\alpha} \Pi^\alpha \bar{G}_a, \forall \bar{G}_a \sim \left[0, \frac{p_t}{dist} \cdot L(\text{dist}) \right] \quad (3)$$

In this formulation, Π^α embodies the product matrix representation, expressed as $\Pi^\alpha = T^\alpha \times \emptyset^\alpha$ within the transmission domain. The term \bar{G}_a symbolizes the Gaussian representation of beamforming with a power ratio of $\frac{p_t}{dist}$. The received signal representation, R_x^α is formulated as $R^\alpha \cdot \Gamma^\alpha \cdot \phi^\alpha$, where Γ^α constitutes the matrix depiction of the received signal R^α at t_x gauged using p_t , $dist$, and $dist_0$. Hence, the Received Reference Signal (RRS) derived from the principal signal signifies the matrix for its ϕ^α . It is crucial to comprehend that for I.C. to attain an elevated ϕ^α , interference must be suppressed to its minimal feasible signal representation. Subsequent to channel estimation, a time-shifted pilot contamination technique has been employed to mitigate communication system challenges. An ensuing sub-section elucidates the application of the time-shifted pilot contamination technique to counteract detrimental effects within the communication paradigm.

3.3 Addressing Pilot Contamination through Compressive Sensing

In an effort to amplify channel cardinality, a pseudo transmitter characterized by a channel gain of zero was introduced. Consequently, the pilot symbols pertaining to all User data were conveyed to the respective base station. In the initial stages, channel gain associated with these pseudo users within a specific coverage area was determined to be zero. Therefore, the compounded signal received by each base station was found to have emanated from both genuine users and contaminators. Harnessing spreader coding techniques tailored to individual users, it was observed that base stations were able to reconstruct the messages directed at both users and contaminators, deploying a compressed sensing renewal algorithm in the process. Remarkably, the non-zero components in the spreader code were discerned to be significantly fewer in number relative to the channel's length " L ". Leveraging this inherent property, certain pilot symbols were successfully achieved with optimal channel estimation outcomes, leading to an enhancement in spectrum utilization, as denoted in Eq. (4):

$$\left\{ \frac{p}{2}, p \text{ is even}; p + \frac{1}{2} p \text{ is odd} \right\} \quad (4)$$

In light of these findings, the count of non-zero elements was methodically deduced from the pertinent channel vector, using the underfitting value " K " as a reference point. Elements within the range L-K were subsequently identified as noise. Consequently, sparsity values were meticulously calibrated within a predetermined range. A notable observation was the preponderance of gain coefficient values within the channel, especially in contrast to the noise amplitude spectrum. Employing differences between proximate elements, a calculation was undertaken to determine the number of elements earmarked for a given iteration, thereby enabling the prediction of sparsity. Elements antecedent to the most pronounced backward difference were selected, being recognized as integral to the support set due to their potential channel information content.

4 Experimental Results and Discussion

This section presents the experimental outcomes based on selected parameters: BER, Computational Time, SNR, and Spectral Efficiency. The results, derived from these parameters, were subsequently benchmarked against two conventional approaches: ILP and QLIC. Emphasis was also placed on evaluating the performance of the proposed DQDA-IC.

- SNR: This metric was calculated as the proportion of signal power to noise power and is typically denoted in decibels. A ratio surpassing 1:1 (or above 0 dB) indicates a predominantly signal-heavy reading. The computation is illustrated in Eq. (5):

$$SNR = \frac{P(\text{signal})}{p(\text{noise})} \quad (5)$$

In Figure 2, an SNR comparison was made between the DQDA-IC and the prevailing ILP and QLIC methods. The horizontal axis marks the number of cells examined, while the vertical axis denotes the percentage of SNR achieved. Notably, the DQDA-IC method recorded an SNR of 63%, surpassing ILP by 5% and QLIC by 7%.

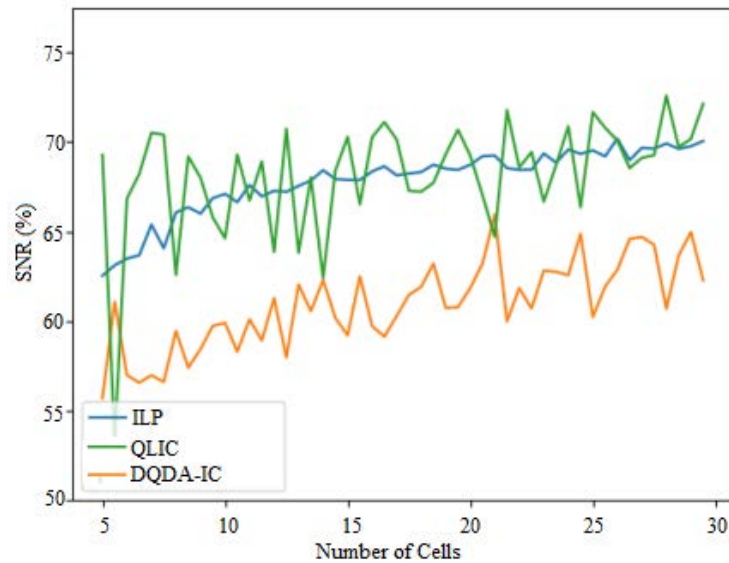


Figure 2. Comparison of Signal to Noise Ratio

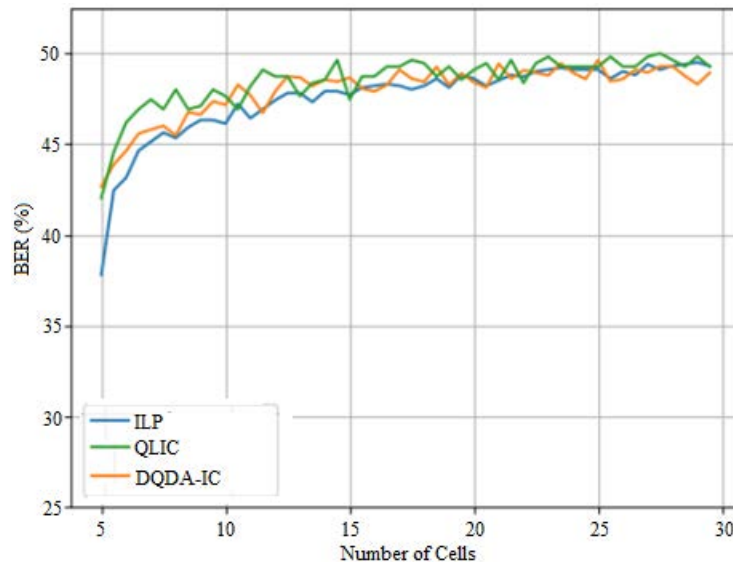


Figure 3. Comparison of Bit Error Rate

- **BER:** This metric was derived by dividing the total errors detected in a bit by the sum of transmitted bits within a specified interval.

In Figure 3, the BER for DQDA-IC was juxtaposed with those of ILP and QLIC. The DQDA-IC method exhibited a BER of 56%, outperforming ILP and QLIC by 3% and 2% respectively.

- **Computational Time:** This metric offers insight into the algorithmic efficiency, reflecting the temporal resources necessary for execution.

A comparative study, illustrated in Figure 4, demonstrated that the DQDA-IC required 40% of the computational time, which proved to be 7% and 5% more efficient than the ILP and QLIC methods, respectively.

- **Spectral Efficiency:** This index elucidates the data throughput achievable within a designated bandwidth in a communication system.

Figure 5 contrasts the spectral efficiency metrics of the DQDA-IC against the ILP and QLIC benchmarks. The DQDA-IC method registered a spectral efficiency of 92%, a modest yet significant 2% and 1% improvement over ILP and QLIC, respectively.

A comprehensive comparative analysis, including all evaluated parameters, is tabulated in Table 1.

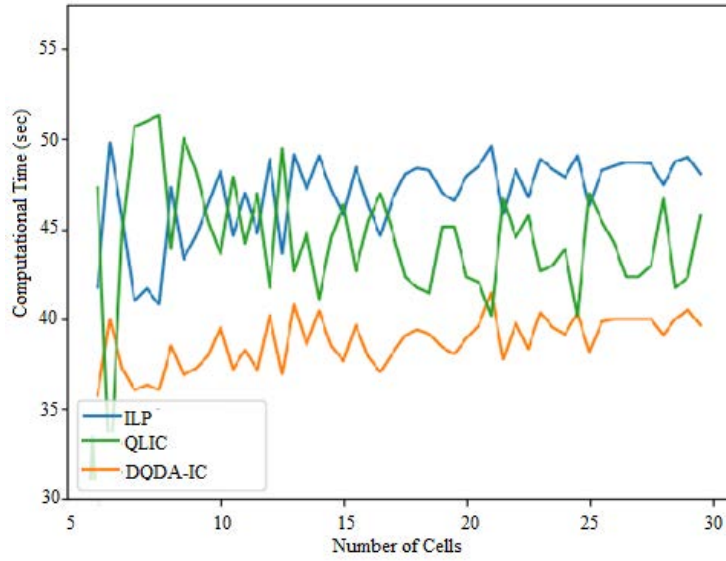


Figure 4. Comparison of computational time

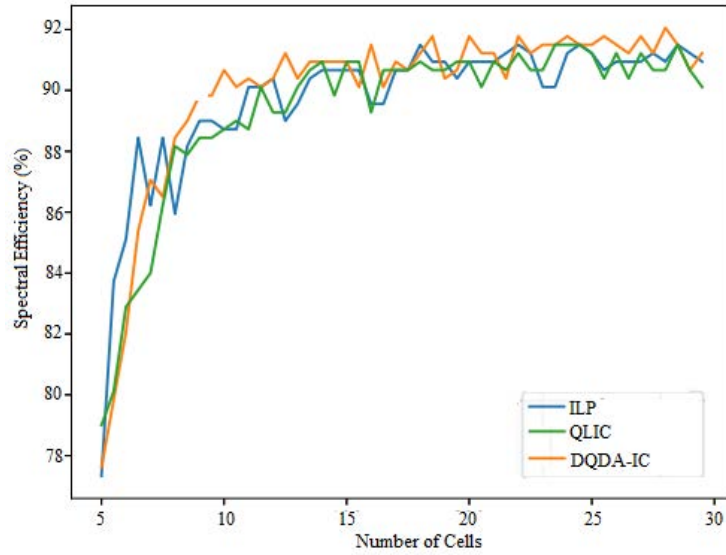


Figure 5. Comparison of spectral efficiency

Table 1. Key parameters of our model

Parameters	ILP [17]	QLIC [18]	DQDA-IC (Proposed)
SNR (%)	68	70	63
BER (%)	59	58	56
Computational Time (ms)	47	45	40
Spectral Efficiency (%)	90	91	92

An examination of these findings suggests that the proposed DQDA-IC, when integrated with MIMO systems, augments network capacity and fortifies data transmission proficiency. Hence, for wireless data-transmission communication systems, the DQDA-IC method emerges as a notably viable option.

5 Conclusions

In wireless communication systems, signal detection performance has been observed to deteriorate considerably due to the dual challenges of inadequate channel estimation affected by received noise and the amplification of this received noise during channel compensation, contingent on channel conditions. Existing channel estimation

methodologies highlight the inherent difficulty in achieving flawless channel estimation, predominantly attributed to pilot contamination caused by the intrusion of received noise. Moreover, even in instances where channel estimation approaches the ideal, the amplification of received noise during channel compensation intensifies noise susceptibility during the demodulation process, which remains contingent upon the channel's state.

Addressing these identified shortcomings, the DQDA-IC was introduced, underpinned by the principles of compressive sensing. This algorithm emerged as an efficacious channel estimation strategy, leveraging available data within wireless communication environments. When benchmarked against conventional methodologies, it was found that DQDA-IC realized 63% in SNR, 56% in BER, and 92% in spectral efficiency, all within a computational timeframe of 40 milliseconds.

Anticipating future research trajectories, attention is being directed towards the integration of deep learning paradigms into channel estimation. This initiative aims to advance pilot contamination models, thereby fostering more robust interference mitigation.

Data Availability

The data used to support the findings of this study are available from the corresponding author upon request.

Conflicts of Interest

The authors declare that they have no conflicts of interest.

References

- [1] X. Zhu and R. D. Murch, "Performance analysis of maximum likelihood detection in a MIMO antenna system," *IEEE Trans. Commun.*, vol. 50, no. 2, pp. 187–191, 2002. <https://doi.org/10.1109/26.983313>
- [2] B. Hassibi and H. Vikalo, "On the sphere-decoding algorithm I. Expected complexity," *IEEE Trans. Commun.*, vol. 53, no. 8, pp. 2806–2818, 2005. <https://doi.org/10.1109/TSP.2005.850352>
- [3] C. J. Huang, C. S. Sung, and T. S. Lee, "A near-ML complex K-best decoder with efficient search design for MIMO systems," in *2010 International Symposium on Intelligent Signal Processing and Communication Systems*, Chengdu, China, 2010, pp. 1–18. <https://doi.org/10.1109/ISPACS.2010.5704617>
- [4] C. Piao, Y. Liu, K. Jiang, and X. Mao, "Dynamic K-best sphere decoding algorithms for MIMO detection," *Commun. Netw.*, vol. 5, no. 3, pp. 103–107, 2013.
- [5] X. Lou, Q. Zhou, Y. Chen, and D. Wu, "Research on low complexity K-best sphere decoding algorithm for MIMO systems," *Wireless Pers. Commun.*, vol. 84, pp. 53–56, 2015. <https://doi.org/10.1007/s11277-015-2648-z>
- [6] X. Guo and S. Yuan, "A new tree pruning SD algorithm to eliminate interference," *Int. J. Digit. Content Technol. its Appl.*, vol. 7, no. 7, pp. 476–482, 2013.
- [7] R. Rahim, S. Murugan, S. Priya, S. Magesh, and R. Manikandan, "Taylor based grey wolf optimization algorithm (TGWAO) for energy aware secure routing protocol," *Int. J. Comput. Netw. Appl.*, vol. 7, no. 4, pp. 93–102, 2020. <https://doi.org/10.22247/ijcna/2020/196041>
- [8] S. Dorner, S. Cammerer, J. Hoydis, and S. ten Brink, "Deep learning based communication over the air," *IEEE J. Sel. Top. Signal Process.*, vol. 12, no. 1, pp. 132–143, 2018. <https://doi.org/10.1109/JSTSP.2017.2784180>
- [9] D. Wubben, R. Bohnke, J. Rinas, V. Kuhn, and K. Kammeyer, "Efficient algorithm for decoding layered space-time codes," *IEEE Electron. Lett.*, vol. 37, no. 22, pp. 1348–1350, 2001.
- [10] D. Wubben, R. Bohnke, V. Kuhn, and K. Kammeyer, "MMSE extension of V-BLAST based on sorted QR decomposition," in *IEEE 58th Vehicular Technology Conference. VTC 2003-Fall (IEEE Cat. No.03CH37484)*, Orlando, FL, USA, 2003, pp. 508–512. <https://doi.org/10.1109/VETEFC.2003.1285069>
- [11] P. Luethi, A. Burg, S. Haene, D. Perels, N. Felber, and W. Fichtner, "VLSI implementation of a high-speed iterative sorted MMSE QR decomposition," in *2007 IEEE International Symposium on Circuits and Systems*, Orleans, LA, USA, 2007, pp. 1421–1424. <https://doi.org/10.1109/ISCAS.2007.378495>
- [12] T. L. Marzetta, "Multi-cellular wireless with base stations employing unlimited numbers of antennas," in *Proc. UCSD Inf. Theory Applicat. Workshop*, 2010.
- [13] T. L. Marzetta, "Noncooperative cellular wireless with unlimited numbers of base station antennas," *IEEE Trans. Wireless Commun.*, vol. 9, no. 11, pp. 3590–3600, 2010. <https://doi.org/10.1109/TWC.2010.092810.091092>
- [14] E. G. Larsson, "Very large MIMO systems: Opportunities and challenges," Linköping University, Tech. Rep., 2012. http://www.kth.se/polopoly_fs/1.303070!/Menu/general/column-content/attachment/Large_MIMO.pdf
- [15] C. Xiong, G. Y. Li, S. Zhang, Y. Chen, and S. Xu, "Energy-and spectral-efficiency tradeoff in downlink OFDMA networks," in *2011 IEEE International Conference on Communications (ICC)*, Kyoto, Japan, 2011, pp. 3874–3886. <https://doi.org/10.1109/icc.2011.5962777>

- [16] F. Rusek, D. Persson, B. K. Lau, E. G. Larsson, T. L. Marzetta, O. Edfors, and F. Tufvesson, "Scaling up MIMO: Opportunities and challenges with very large arrays," *IEEE Signal Process. Mag.*, vol. 30, no. 1, pp. 40–46, 2013. <https://doi.org/10.1109/MSP.2011.2178495>
- [17] K. Wang, F. R. Yu, L. Wang, J. Li, N. Zhao, Q. Guan, B. Li, and Q. Wu, "Interference alignment with adaptive power allocation in full-duplex-enabled small cell networks," *IEEE Trans. Veh. Technol.*, vol. 68, no. 3, pp. 3010–3015, 2019. <https://doi.org/10.1109/TVT.2019.2891675>
- [18] S. J. Jang and S. J. Yoo, "Q-learning-based dynamic joint control of interference and transmission opportunities for cognitive radio," *EURASIP J. Wirel. Commun. Netw.*, vol. 2018, no. 1, pp. 1–24, 2018. <https://doi.org/10.1186/s13638-018-1155-9>
- [19] H. Q. Ngo, E. G. Larsson, and T. L. Marzetta, "Energy and spectral efficiency of very large multiuser MIMO systems," *IEEE Trans. Commun.*, vol. 61, no. 4, pp. 1436–1449, 2013. <https://doi.org/10.1109/TCOMM.2013.020413.110848>
- [20] G. Y. Li, Z. K. Xu, C. Xiong, C. Y. Yang, S. Q. Zhang, Y. Chen, and S. G. Xu, "Energy-efficient wireless communications: Tutorial, survey, and open issues," *IEEE Wirel. Commun. Mag.*, vol. 18, no. 6, pp. 28–35, 2011. <https://doi.org/10.1109/MWC.2011.6108331>
- [21] C. Xiong, G. Y. Li, S. Zhang, Y. Chen, and S. Xu, "Energy-and spectral-efficiency tradeoff in downlink OFDMA networks," *IEEE Trans. Wireless Commun.*, vol. 10, no. 11, pp. 3874–3886, 2011. <https://doi.org/10.1109/TWC.2011.091411.110249>
- [22] F. Rosário, F. A. Monteiro, and A. Rodrigues, "Fast matrix inversion updates for massive MIMO detection and precoding," *IEEE Signal Process. Lett.*, vol. 23, no. 1, pp. 75–79, 2016. <https://doi.org/10.1109/LSP.2015.2500682>
- [23] K. V. Vardhan, S. K. Mohammed, A. Chockalingam, and B. S. Rajan, "A low-complexity detector for large MIMO systems and multicarrier CDMA systems," *IEEE J. Sel. Areas Commun.*, vol. 26, no. 3, pp. 473–485, 2008. <https://doi.org/10.1109/JSAC.2008.080406>
- [24] P. Li and R. D. Murch, "Multiple output selection-LAS algorithm in Large MIMO systems," *IEEE Commun. Lett.*, vol. 14, no. 5, pp. 399–401, 2010. <https://doi.org/10.1109/LCOMM.2010.05.100092>